Absorption Spectra of Ground-State and Low-Lying Electronic States of Copper Nitrosyl: A Rare Gas Matrix Isolation Study

Lahouari Krim,[†] Xuefeng Wang,[‡] Laurent Manceron,*[,†] and Lester Andrews[‡]

Université Pierre et Marie Curie-Paris 6, CNRS UMR 7075, LADIR, case 49, 4 place Jussieu 75252 Paris, France, and Department of Chemistry, University of Virginia, Box 400319, Charlottesville, Virginia 22901-4319

Received: July 9, 2005; In Final Form: September 16, 2005

The reaction of ground-state Cu atoms with NO during condensation in solid argon, neon, and binary argon/neon mixtures has been reinvestigated. In addition to the ground-state already characterized in rare gas matrixes by its ν_1 mode in reactions of laser-ablated Cu with nitric oxide, another very low lying electronic state is observed for CuNO in solid argon. Photoconversion and equilibrium processes are observed between the two lowest lying electronic states following photoexcitations to second and third excited states in the visible and near-infrared. The electronic spectrum of the CuNO complex was also recorded to understand the photoconversion processes. In solid neon, only the ground state (probably $^1A'$) and the second and third excited states are observed. This suggests that interaction with the argon cage stabilizes the triplet state to make $^1A'$ and $^3A''$ states almost isoenergetic in solid argon. On the basis of previous predictions founded on DFT calculations on the very low lying $^1A'$ and $^3A''$, a mechanism is proposed, involving the singlet−triplet state manifolds. For these two lower and one higher electronic states, $^{14}N/^{15}N$, $^{16}O/^{18}O$, and $^{63}Cu/^{65}Cu$ isotopic data on ν_1, ν_2, and ν_3 have been measured. On the basis of harmonic force-field calculations and relative intensities in the vibronic progressions, some structural parameters are estimated. The molecule is bent in all electronic states, with Cu−N−O bond angles varying slightly around 130 ± 10°, but the Cu−N bond force constants are substantially different, denoting larger differences in bond lengths.

1. Introduction

The interest of modeling metal−ligand interactions in well-defined "model" systems such as the interaction of isolated metal atoms and molecular ligands stems from the need to characterize spectroscopic markers or to test theoretical models before studying more complex systems, such as chemisorption processes of small adsorbates such as NO or CO on metal surfaces or supported metal-containing species.[1−3] This has motivated both theoretical and experimental studies on related zerovalent metal atom−molecule complexes. In particular, the interaction of Cu atoms with NO has been the object of several experimental and theoretical studies, leading to different results or predictions. About 10 years ago, Sülzle et al.[4] presented experimental evidence for the existence of neutral and cationic CuNO in the gas phase. In a theoretical investigation at the CCSD(T) level, Hrusak et al.[5] predicted that CuNO should have an end-on structure with a bonding energy of 10.5 kcal/mol in the $^1A'$ state, while the related triplet was calculated to be approximately half as stable; however, at CISD or CCSD levels, the ordering was reversed. Matrix isolation work by Chiarelli and Ball[6,7] identified next the CuNO species through two IR absorptions at 1610 and 608 cm^{-1} in solid argon, following the reaction of Cu atoms with NO. These assignments were revised in the recent study of Zhou and Andrews,[8] who demonstrated with mixed isotopic NO that the carrier of these absorptions was the dinitrosyl species $Cu(NO)_2$, while the CuNO species could be identified through one vibrational mode, the ν_1 NO-stretching mode near 1587 and 1602 cm^{-1} in argon and neon, respectively. Another absorption was observed near 1520 cm^{-1} in solid argon in this latter study, which could not be assigned to charged species ($CuNO^{\pm}$) but revealed the presence of a single nitrosyl group as well. Other theoretical studies meanwhile reinvestigated the electronic structure of the CuNO species. Barone and Adamo[9] used hybrid density functional/Hartree−Fock methods and concluded also that the complex should have a bent shape and a substantial binding energy (16 kcal/mol), but with a $^3A''$ ground state, the $^1A'$ state lying some 2 kcal/mol above. Salahub and co-workers,[10] using pure DFT methods, found a reverse ordering and again a $^1A'$ ground state.

The goal of the present study is 4-fold: (i) use different experimental methods to scale up preferentially the quantity of the neutral compounds and enhance the detectivity in the low-frequency region to obtain a complete vibrational spectrum for CuNO, (ii) compare the vibrational data and the derived geometrical properties to the current predictions of quantum chemical calculations, (iii) assess the nature of the first electronic states of matrix-isolated CuNO and propose a scheme for the observed photophysical process, and (iv) examine the influence of the rare gas matrix on the electronic structure of CuNO.

2. Experimental Section

The Cu + NO samples were prepared by cocondensing Cu vapor and NO/rare gas (RG) mixtures (0.1−4% molar ratios) onto a cryogenic metal mirror maintained at either 4 K (neon) or 10 K (argon). The experimental methods and setup have been previously described.[11] Briefly, here, a tungsten filament mounted in a furnace assembly and wetted with copper (Alpha Inorganics, 99.995%) was heated resistively from 1000 to 1300 °C to generate a beam of Cu vapor. Metal deposition rates, monitored with a microbalance, were typically of the order of

[†] Université Pierre et Marie Curie.
[‡] University of Virginia.

10.1021/jp053778l CCC: $30.25
Published on Web 10/21/2005

0.1−10 μg/min. Deposition times were around 90 min. Argon or neon gas was furnished by Air Liquide with a purity of 99.999%. ^{14}NO gas was also provided by Air Liquide, but with a stated chemical purity of 99.9%, and ^{15}NO gas from Isotec had an isotopic purity of 97.8%. $^{14}N^{18}O$ was prepared in the laboratory by addition of $^{18}O_2$ onto $^{14}N^{16}O$ gas to form $^{14}N^{(16+18)}O_2$, which was subsequently reduced to $^{14}N^{18}O$ and $^{14}N^{16}O$ by reaction with mercury.[12] The resulting gas is a mixture containing approximately 52% $^{14}N^{16}O$ and 48% $^{14}N^{18}O$. In all samples, NO gas and its isotopomers were purified, to remove N_2, N_2O, and NO_2, by using trap-to-trap vacuum distillations. The purity of samples was confirmed spectroscopically.

In general, infrared and UV−visible spectra of the resulting sample were recorded in the transmission-reflection mode between 30 000 and 70 cm^{-1} using a Bruker 120 FTIR spectrometer and suitable combinations of TiO_2/quartz, CaF_2/Si, KBr/Ge, or composite beam splitters with either Si, InGaAs, liquid N_2 cooled InSb photodiodes, or narrow band HgCdTe photoconductor, or a liquid He-cooled Si−B bolometer, fitted with cooled band-pass filters. The resolution was varied between 0.05 and 1 cm^{-1}. Bare mirror backgrounds, recorded from 30 000 to 70 cm^{-1} prior to sample deposition, were used as references in processing the sample spectra. Also, absorption spectra in the UV−visible and near-, mid- and far-infrared were collected on the same samples through either CaF_2, KBr, or polyethylene windows mounted on a rotatable flange separating the interferometer vacuum (10^{-3} mbar) from that of the cryostatic cell ($<10^{-7}$ mbar). The spectra were subsequently subjected to baseline correction to compensate for infrared light scattering and interference patterns.

It was found that some photoprocesses could be initiated by UV−visible or near-infrared light, and selective excitations were first performed in the visible and UV ranges using a 200 W mercury−xenon high-pressure arc lamp and either interference narrow (10 nm fwhm) or broad band filters. Next, narrow band photoexcitations (5−6 cm^{-1} line width) were performed over a wider range using the idler beam of an OPO source operating with a BBO crystal, pumped by the third harmonics of a Nd:YAG laser (OPOTEK, QUANTEL), delivering 0.5−0.2 mJ light pulses at 20 Hz, continuously tunable in the 12 500−4300 cm^{-1} range. Next, or after sample annealing up to 12K (neon) or 35 K (argon) in several steps, spectra of the samples were recorded again between 30 000 and 70 cm^{-1} as outlined above.

3. Results

a. Vibrational Spectra of CuNO. *Cu + NO in Argon*. In samples where Cu atoms were co-deposited with relatively dilute NO/Ar mixtures, infrared spectra in the metal nitrosyl N−O stretching region (1300−1900 cm^{-1}) presented three groups of absorptions in addition to those attributed to unreacted NO, $(NO)_2$, and their isotopomers. These absorptions can be detected near 1611, 1587, and 1520 cm^{-1} (Figure 1) even in diluted samples. After studying the variation of these signals over a wide concentration range, it appears that they all presented either linear or quadratic dependences in Cu or NO. The two lower groups near 1520 and 1587 cm^{-1} presented a first-order dependence with respect to the metal atom concentration and a first-order dependence with respect to the NO concentration. The band at 1587 cm^{-1} has been previously assigned to the CuNO species in the recent laser ablation study.[8] In the present study, we found that both groups presented a linear concentration dependence in either reagent and thus correspond to molecular species containing one Cu atom and one NO molecule. Each

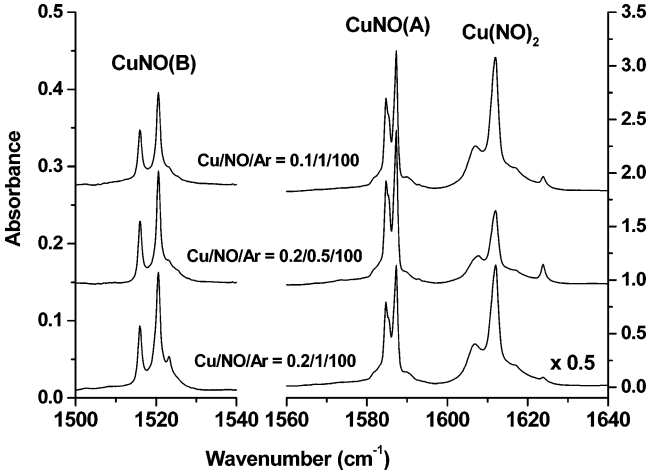

Figure 1. Infrared spectrum in the 1640−1500 cm^{-1} nitrosyl stretching region for various Cu/NO/Ar concentrations.

group is split into several components, the main ones being located at 1520.6, 1516.0 cm^{-1} and at 1587.4, 1584.7 cm^{-1}, respectively. The multiplet components evolved always in parallel during the concentration studies, but they exhibited some relative intensity changes when annealing the matrixes, a behavior typical for trapping site effects in solid matrixes.

Finally, the signal detected around 1611 cm^{-1} presents first- and second-order dependencies in Cu and NO, respectively, in full agreement with the conclusions of Zhou and Andrews,[8,13] who assigned this band to a $Cu(NO)_2$ species.

New information relative to the copper-mononitrosyl species will now be discussed. The samples were quite deeply colored and presented marked photosensitivity. First exposure to UV−visible light resulted in a small decrease of the CuNO band, and a small parallel increase in $Cu(NO)_2$, showing that the CuNO could be photolyzed and that subsequent diffusion of the transitionally hot fragments is thus taking place. After this initial effect, a qualitatively different process can be observed: irradiating the sample with either green or near-infrared light produced a notable effect on the CuNO 1587.4 cm^{-1} band as well as on the unidentified absorption near 1520.6 cm^{-1}. Immediately after the irradiation, the 1587.4 cm^{-1} band decreased by as much as 40%, while the 1520.6 cm^{-1} absorption presented a small increase, mainly as a new shoulder on the low-frequency side. Continuous observation of the sample next showed that, after about 5 min, the 1587.4 cm^{-1} band had recovered 70% of its initial intensity, while the 1520.6 cm^{-1} band decreased conversely. After 10 min, both bands had almost recovered their initial intensities. Such an effect is illustrated in Figure 2 for irradiation at 632 nm of a sample pre-exposed to broad band visible light to remove the irreversible processes. The process is then fully reversible and was repeated several times on each sample. It thus shows that the bands at 1587.4 and 1520.6 cm^{-1} correspond to two different states of the CuNO complex. The photophysical process has been studied more quantitatively by acquiring one scan every 30 s, starting immediately after sample irradiation of the matrix, and by studying the kinetic behavior of either band. The experiment could be repeated several times, varying the sample temperature between 9 and 20 K to evidence a possible thermal activation, but no temperature dependence could be evidenced within this limited temperature range. As stated before, the photoexcitation could be achieved at several wavelengths between 540 and 2000 nm, but irradiation in the red near 632 nm and in the infrared near 1700 nm were most effective. The decay of the CuNO(B) bands, after their initial growth just after the irradiation, could

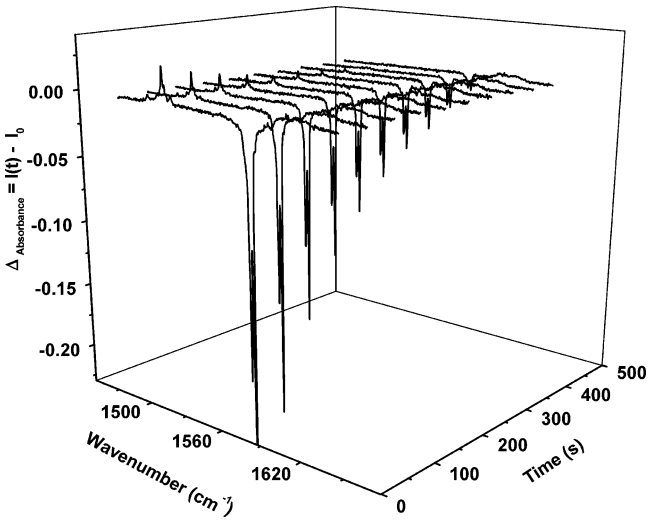

Figure 2. Photoconversion between the two low-lying states of CuNO in argon matrix monitored in the nitrosyl stretching region for both states. I_0: spectrum taken before matrix irradiation, $I(t)$: spectra taken "t" seconds after 5-min irradiation at 632 nm.

be fitted to a simple exponential decline of the type $I_B = I_{B0}(1 + e^{-t/\tau_B})$, where I_B is the integrated intensity of the CuNO(B), I_{B0} the initial integrated intensity before irradiation, and τ_B is the rate of the decline. Conversely, the CuNO(A) bands, which had initially decreased after the initial irradiation, recovered their initial intensities with an increasing exponential curve of the type $I_A = I_{A0}(1 - e^{-t/\tau_A})$, where I_A is the integrated intensity of a band attributed to CuNO(A), I_{A0}, the initial integrated intensity before irradiation, and τ_A is the rate of the growth. Spectra obtained following a selective photoirradiation show a conversion between the two CuNO low-lying electronic states. The measured conversion rate constant ($\tau_A = \tau_B$) does not depend on the temperature of the matrix below 30 K and is found to be equal to 300 ± 10 s.

From the linear relationship between the intensities of the A and B νNO bands, a ratio between the extinction coefficients ($p = \epsilon_B/\epsilon_A$) of 0.09 is deduced, which shows a large difference in transition moments for the nitrosyl stretching modes in the A and B states. Knowing this ratio, we are able to calculate the population ratio of the two low-lying states. The ratio does not vary noticeably if the matrix temperature is changed in the 8−25 K range and is about 1.2 ± 0.1 in the dark (which shows that the A and B states are nearly degenerate) and about 3.0 ± 0.1 after irradiation, in our experimental conditions. The initial balance is restored in the dark.

Samples obtained with varying concentrations of NO and Cu in the argon matrix present, on one hand, four bands located at 3141.7, 895.6, 452.6, and 278.2 cm^{-1}, whose relative intensities remain constant with respect to the 1587.4 cm^{-1} band (set A) throughout concentration, annealing, and photophysical effects. Also, three other bands are located near 3012, 512, and 219 cm^{-1}, whose relative intensities have the same behavior as the 1520 cm^{-1} band (set B).

Each of these bands appears as a doublet in spectra obtained with NO isotopic mixtures ($^{14}N^{16}O/^{15}N^{16}O$ or $^{14}N^{16}O/^{14}N^{18}O$; see Figures 3−5 and Table 1), as expected for mononitrosyl species.

The band located at 3141.7 cm^{-1} is consistent with the first overtone of the band located at 1587.4 cm^{-1} (Figure 3). The integrated intensity for 3141.7 cm^{-1} is about 46 times smaller than that of the fundamental band, and the isotopic shifts are nearly twice the shifts observed for the corresponding fundamental band. From the knowledge of fundamental and overtone frequencies, the X_{11} anharmonicity constant has been evaluated at −16.5, −15.5, and −14.6 cm^{-1} for $Cu^{14}N^{16}O$(A), $Cu^{15}N^{16}O$-(A), and $Cu^{14}N^{18}O$(A), respectively. The low-frequency absorptions appear as doublets due to the copper natural isotopic distribution (^{65}Cu 31%, ^{63}Cu 69%) which can be resolved using 0.1 cm^{-1} resolution (Figure 4). For the ^{63}Cu isotopic species, the band at 452.6 cm^{-1} is shifted to 440.4 and 450.1 cm^{-1} upon replacing $^{14}N^{16}O$ by $^{15}N^{16}O$ and $^{14}N^{18}O$, respectively. A weak band located at 895.6 cm^{-1} can be assigned to the first overtone of the 452.6 cm^{-1} fundamental. From the knowledge of fundamental and overtone frequencies, the X_{22} anharmonicity constant can be evaluated at −4.8, −4.5, and −5.0 cm^{-1} for $Cu^{14}N^{16}O$(A), $Cu^{15}N^{16}O$(A), and $Cu^{14}N^{18}O$(A), respectively. The band at 278.2 cm^{-1} is shifted to 276.6 and 269.2 cm^{-1} (Figure 4), with these same precursors.

The absorptions observed for the different isotopic species of CuNO(B) are listed in Table 2. The band near 1520 cm^{-1} is also doublet (1520.6/1516.0 cm^{-1}), due to matrix site effects, and experiences a relatively large shift with ^{18}O substitution and a smaller one with ^{15}N, to 1482.5/1477.5 and 1492.8/1488.3 cm^{-1}, respectively (Figure 3). A weaker band is observed also as a doublet at 3012.9/3003.3 cm^{-1}, which corresponds to the first overtone of the former mode, given the frequencies and isotopic shifts. The X_{11} anharmonicity constant has been evaluated, for each site in the matrix, at −14.15/−14.35, −13.4/−13.6, and −12.9/−12.7 cm^{-1} for $Cu^{14}N^{16}O$(B), $Cu^{15}N^{16}O$-(B), and $Cu^{14}N^{18}O$(B), respectively. The $^{63}Cu/^{65}Cu$ isotopic shift for the band near 512 is much larger than that observed for CuNO(A) bands (see Figures 4 and 5), while the Cu isotopic structure for the low-frequency absorption near 219.5 cm^{-1} appears unresolved even at 0.1 cm^{-1} resolution. All the isotopic data are reported in Tables 1 and 2.

Cu + NO in Neon. In samples where Cu atoms were co-deposited with NO/Ne, only one set of bands assignable to CuNO is detected. Figure 6 compares the IR spectra of samples obtained in identical conditions in argon and in neon matrixes. For the NO stretching mode, the band is 0.8% blue-shifted in neon matrix. The ν_2 and ν_3 modes are observed at 452.1 and 276.4 cm^{-1}, respectively, almost at the same energies in neon and in argon matrixes. Thus, the observed bands correlate with the bands attributed to state A of CuNO complex isolated in solid argon. The B state is not observed in solid neon, even after photoexcitation.

Cu + NO in Mixed Argon/Neon Matrixes. Two mixed neon−argon experiments were performed in an attempt to observe the 1520 cm^{-1} argon matrix feature (state B).

An experiment with 2% Ar and 0.1% NO in neon gave broadened CuNO absorptions at 1596 cm^{-1} but no feature near 1520 cm^{-1}. However, annealing increased the $Cu(NO)_2$ bands at the expense of CuNO absorptions and produced a weak new 1523.4 cm^{-1} feature (state B). In the experiment with 5% Ar and 0.1% NO in neon, a weak band is directly observed at 1523.4 cm^{-1}. Annealing to 10 and 13 K matched the observed bands in the direction of their argon matrix counterparts, and annealing to 19 K, which removed most of the neon, left sharp, weaker 1587.4 and 1520.6 cm^{-1} bands in very close agreement with pure argon matrix values for copper nitrosyl species. Annealing allowed argon to replace neon stepwise in the intimate solvation shell, and argon matrix counterparts were produced after evaporation of the neon (19 K annealing). The broad 1523.4 cm^{-1} absorption became a sharp 1520.6 cm^{-1} band (state B) after evaporation of neon, identical to the pure argon product. The state B can be observed only if argon atoms are

TABLE 1: Observed Frequencies (in cm^{-1}) for the $^{63}Cu^{14}N^{16}O$, $^{65}Cu^{14}N^{16}O$, $^{63}Cu^{15}N^{16}O$, and $^{63}Cu^{14}N^{18}O$ Isotopic Species of Copper Mononitrosyl (state A) Isolated in an Argon Matrix

assignment	$^{63}Cu^{14}N^{16}O$	$^{65}Cu^{14}N^{16}O$	$^{63}Cu^{15}N^{16}O$	$^{65}Cu^{15}N^{16}O$	$^{63}Cu^{14}N^{18}O$	$^{65}Cu^{14}N^{18}O$
$2\nu_1$ site 1	3141.7 (0.022)[a]	3141.7	3088.2		3060.8	
ν_1 site 1	1587.37	1587.37	1559.55		1544.96	
ν_1 site 2	1584.7 (1.0)	1584.7	≈1558		≈1543.5	
$2\nu_2$ site 1	895.6 (0.0007)		871.7		890.2	
ν_2 site 1	452.60	452.05	440.37	439.04	450.11	449.6
ν_2 site 2	451.8 (0.015)	451.2	439.8		449.3	
ν_3 site 1	278.23	277.13	276.55	275.5	269.15	268.1
ν_3 site 2	277.68 (0.0055)	276.58	276.02		268.60	

[a] Relative intensities with respect to the strongest fundamental are in parentheses.

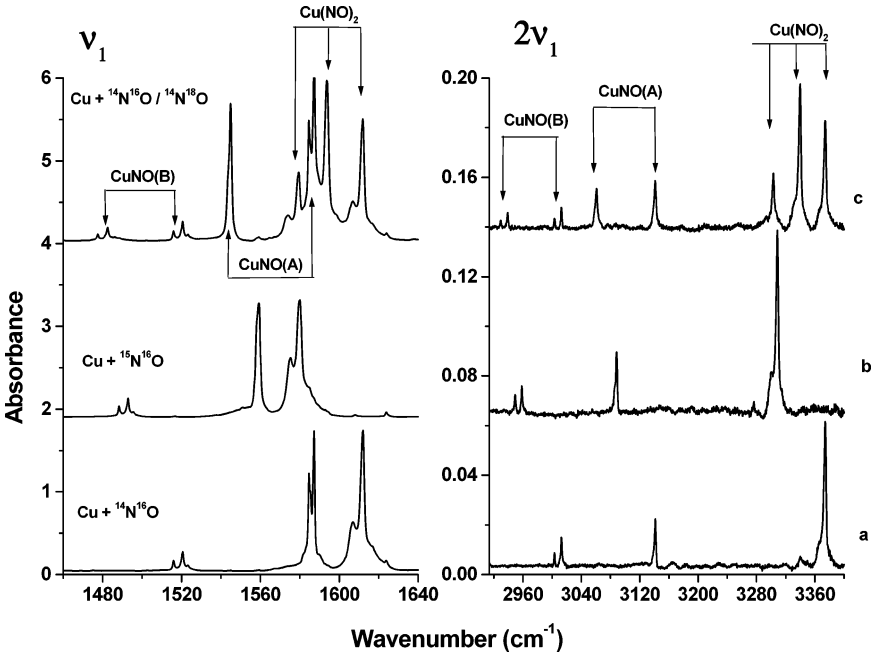

Figure 3. Infrared spectrum in the ν_1 and $2\nu_1$ region of CuNO and $Cu(NO)_2$: (a) $Cu/^{14}N^{16}O/Ar = 0.2/1/100$, (b) $Cu/^{15}N^{16}O/Ar = 0.2/1/100$, (c) $Cu/^{14}N^{16}O/^{14}N^{18}O/Ar = 0.2/0.6/0.4/100$).

added in the neon matrix, which indicates that B is stabilized only in an argon matrix.

Vibrational Analysis. The products of the nitric oxide and copper cocondensation reaction, as described previously, showed the coexistence in solid argon of two low-lying CuNO electronic states: CuNO(A) with vibrational transitions at 278.2, 452.6, 895.6, 1587.4, and 3141.7 cm^{-1}, and CuNO(B), with vibrational transitions at 219.5, 512.1, 1520.6, and 3012.9 cm^{-1}.

Three fundamental bands pertaining to CuNO(A) have been measured at 1587.4, 452.6, and 278.2 cm^{-1}. Among these absorptions, the 1587.4 cm^{-1} band had been formerly assigned to the NO stretching vibration of CuNO ($^1A'$) ν_1.[8] This band shifts to lower frequency by 27.8 cm^{-1} when the $^{15}N^{16}O$ is used and by 42.4 cm^{-1} in the case of $^{14}N^{18}O$. The difference between the $^{14}N/^{15}N$ and $^{16}O/^{18}O$ isotopic effects on ν_1 for CuNO(A) (1559.6 − 1545.0 = 14.6 cm^{-1}) and PdNO (1630.7 − 1617.6 = 13.1 cm^{-1}) species are rather similar.[14] In both cases, the effect of $^{16}O/^{18}O$ substitution is more important than that of $^{14}N/^{15}N$. That is not the case for other systems, such as the related NiNO ($^2A'$) species,[15] where the of $^{14}N/^{15}N$ isotopic effect is almost identical to that of $^{16}O/^{18}O$ substitution (1643.9 − 1640.9 = 3 cm^{-1}). This indicates a much reduced coupling between the M−NO and N═O coordinates in PdNO and CuNO(A) compared to NiNO. Two parameters can be at the origin of this effect: a Ni−N force constant larger than the Cu−N one, or a smaller value of the bond angle in CuNO causing a decrease in the off-diagonal **G**-matrix element. These two parameters will be compared later.

The 452.6 cm^{-1} band shifts to lower frequency by 12.2 cm^{-1} when $^{14}N^{16}O$ is substituted by $^{15}N^{16}O$, while substitution of $^{14}N^{16}O$ by $^{14}N^{18}O$ causes a smaller shift, about 2.5 cm^{-1}. Conversely, the lower frequency mode shows a smaller shift with $^{15}N^{16}O$ than with $^{14}N^{18}O$ (1.7 vs 9.1 cm^{-1}). The 452.6 cm^{-1} band is about 3 times more intense than the lower frequency band. These two absorptions are attributed to metal−nitrosyl stretching and bending vibrations of CuNO(A), respectively.

For the B state, the three observed fundamental bands have been measured at 1520.6, 512.1, and 219.5 cm^{-1}. The absorption at 1520.6 cm^{-1} band could be attributed to the NO stretching vibration of CuNO(B), ν_1. As in the case of CuNO(A) species, this band shifts to lower frequency exactly by 27.8 cm^{-1} when the $^{15}N^{16}O$ is used and by 38.1 cm^{-1} in the case of $^{14}N^{18}O$. There is a 30% difference between the $^{14}N/^{15}N$, $^{16}O/^{18}O$ substitution effects on the frequencies of the ν_1 mode of CuNO-(A) (1559.6 − 1545.0 = 14.6 cm^{-1}) and those for CuNO(B)

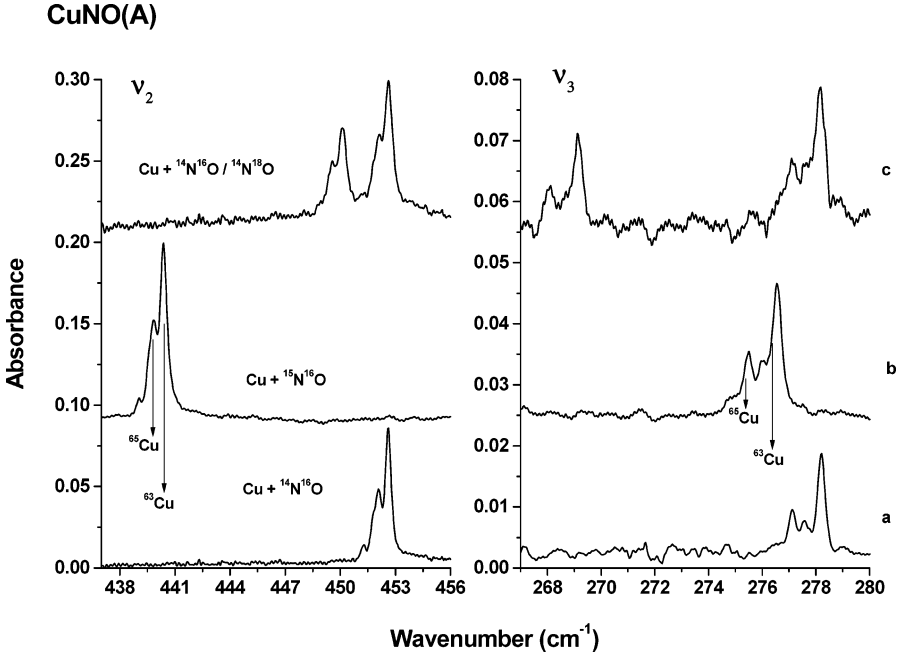

Figure 4. Infrared spectrum in the ν_2, ν_3 region of CuNO(A): (a) Cu/^{14}N^{16}O/Ar = 0.2/1/100, (b) Cu/^{15}N^{16}O/Ar = 0.2/1/100, (c) Cu/^{14}N^{16}O/^{14}N^{18}O/Ar = 0.2/0.6/0.4/100).

TABLE 2: Observed Frequencies (in cm^{-1}) for the ^{63}Cu^{14}N^{16}O, ^{65}Cu^{14}N^{16}O, ^{63}Cu^{15}N^{16}O, and ^{63}Cu^{14}N^{18}O Isotopic Species of Copper Mononitrosyl (state B) Isolated in an Argon Matrix

assignment	^{63}Cu^{14}N^{16}O	^{65}Cu^{14}N^{16}O	^{63}Cu^{15}N^{16}O	^{65}Cu^{15}N^{16}O	^{63}Cu^{14}N^{18}O	^{65}Cu^{14}N^{18}O
$2\nu_1$ site 1	3012.9	id	2958.8	id	2939.2	id
$2\nu_1$ site 2	3003.3 (0.053)[a]		2949.4		2929.6	
ν_1 site 1	1520.6	id	1492.8	id	1482.5	id
ν_1 site 2	1516.0 (1.0)		1488.3		1477.5	
ν_2	512.1 (0.037)	510.2	501.5	499.8	507.9	506.1
ν_3	219.5 (0.037)	≈219.3	216.4	id	214.6	id

[a] Relative intensities with respect to the strongest fundamental are in parentheses.

(1492.8 − 1482.5 = 10.3 cm^{-1}). That indicates a small structural difference between the two A and B states.

The 512.1 cm^{-1} band shifts to lower frequency by 10.6 cm^{-1} when ^{14}N^{16}O is substituted by ^{15}N^{16}O, while substitution of ^{14}N^{16}O by ^{14}N^{18}O causes a smaller shift, about 4.2 cm^{-1} (as in the CuNO(A) case). However, the lower frequency mode shows nearly similar shift with both ^{15}N^{16}O and ^{14}N^{18}O molecules (3.1 vs 5.2 cm^{-1}). The 512.1 cm^{-1} band is as intense as the lower frequency band. These two absorptions are attributed to metal−nitrosyl stretching and bending vibrations of CuNO(B), respectively. The ν_3 frequency mode of CuNO(A) is 21% higher (278.2 vs 219.5 cm^{-1}) than the one of CuNO(B), but the sum of the two lower frequencies corresponding to metal−nitrosyl stretching and bending vibrations [452.6 + 278.2 = 730.8 cm^{-1} for CuNO(A) and 512.1 + 219.5 = 731.6 cm^{-1} for CuNO(B)] is the about same in both A and B low-lying electronic states.

The results of the most recent theoretical studies, which have calculated the three fundamental frequencies for CuNO in the ground ^{1}A′ or ^{3}A″ states, are given in Table 3. Salahub et al.[10] predict that ^{1}A′ is the ground state, using the DFT/BPW method, while DFT calculations done by Andrews et al.[8] show the ground state to be ^{3}A″, using B3LYP, and ^{1}A′, using BP86. In both calculations the energy difference between the two states is predicted to be about 3 kcal/mol.

Experimental measurements show that frequencies of the B state NO stretching and the CuNO bending modes are red-shifted, with respect to A state, by 4% and 21% respectively, while the frequency of the Cu−N stretching mode is blue-shifted by 13%. DFT calculations give the same trends for the NO stretching (−3 to − 5%) and the CuNO bending modes (−20%) between the ^{1}A′ and ^{3}A″ states. On this basis, A could be assigned to the ^{1}A′ state and B to the ^{3}A″ state. However a discrepancy remains, as the ν_2 (mainly Cu−N stretching) frequencies are poorly reproduced. Indeed, these same calculations predict for the ν_2 mode frequency a red shift from 7 to 12% from ^{3}A″ to ^{1}A′, whereas experimental measurements give a blue shift (about 13%) from B to A state. This suggests that the description of the singlet or triplet states is still problematic, and an unambiguous attribution of A and B low-lying electronic states is still pending. The present evidence favors identification of A as the ^{1}A′ and its observation in solid neon as the ground state.

Semiempirical harmonic force field calculations were performed to provide a quantitative basis to the discussion of bonding properties and molecular shape of the A and B CuNO. First, as a starting point we used for state A and B the equilibrium geometries calculated in ref 8: r_{NO} = 1.17 Å, r_{CuN} = 1.94 Å, and ∠CuNO = 119° for ^{1}A′ state and r_{NO} = 1.19 Å, r_{CuN} = 1.89 Å, ∠CuNO = 130° for ^{3}A″ state. Next, to test the geometry, we varied the CuNO bond angle stepwise between 180 and 80° (keeping the bond lengths constant). For each given bond angle value, the potential constants are readjusted to give

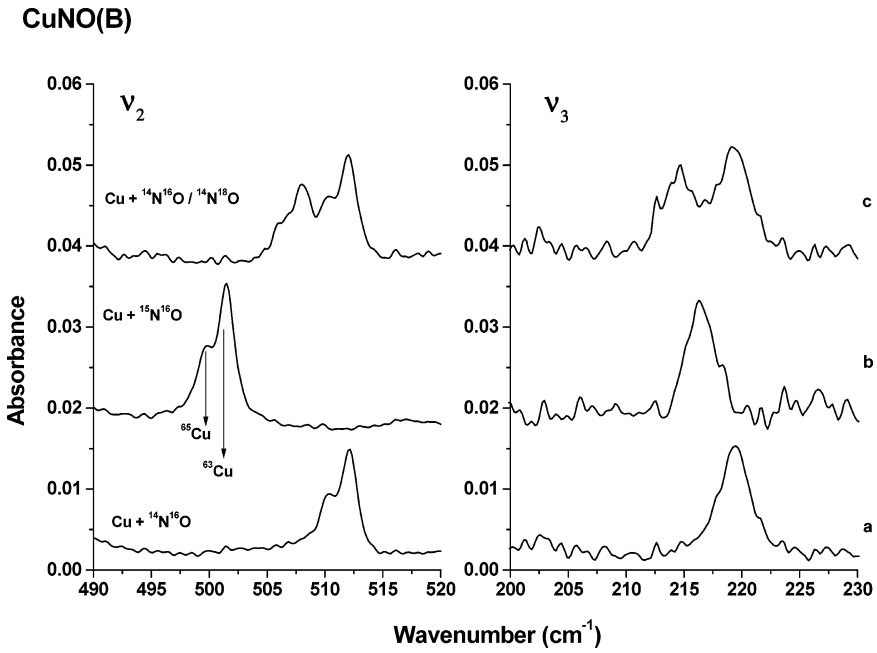

Figure 5. Infrared spectrum in the ν_2, ν_3 region of CuNO(B) (a) Cu/^{14}N^{16}O/Ar = 0.2/1/100, (b) Cu/^{15}N^{16}O/Ar = 0.2/1/100, (c) Cu/^{14}N^{16}O/^{14}N^{18}O/Ar = 0.2/0.6/0.4/100.

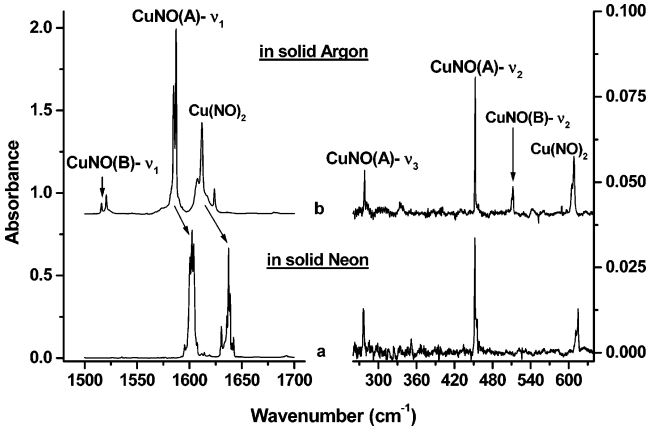

Figure 6. Infrared spectrum in the ν_2, ν_3 region of CuNO: (a) in neon and (b) in argon.

TABLE 3: Observed Anharmonic Frequencies for ^{63}Cu^{14}N^{16}O Isolated in Solid Argon and Calculated Harmonic Frequencies (cm^{-1}) Using Density Functional Methods

	molecule	NO stretch	CuN stretch	CuNO bend
DFT/B3LYP[a]	CuNO ^{1}A	1703.3	470.9	281.3
	CuNO ^{3}A	1618.3	412.1	223.8
shift[b]		−5%	−12.5%	−20.4%
experiment	CuNO(A)	1587.4	452.6	278.2
	CuNO(B)	1520.6	512.1	219.5
shift[c]		−4%	+13%	−21.1%
DFT/BP86[a]	CuNO ^{1}A	1650.2	486.6	292.1
	CuNO ^{3}A	1596.2	450.9	232.5
shift[b]		−3.3%	−7%	−20.4%

[a] From ref 8. [b] Relative shift between ^{3}A″ and ^{1}A′. [c] Relative shift between B and A.

the best overall agreement with the experimental isotopic shifts (^{14}N^{16}O/^{15}N^{16}O and ^{14}N^{16}O/^{14}N^{18}O) on all three (ν_1, ν_2, and ν_3) modes. The best results are obtained for a bond angle in the vicinity of 130 ± 10° for both states, and the isotopic shifts are thus fitted within 0.3 and 1.0 cm^{-1}, for A and B, respectively. Test calculations were performed supposing an O-bonded, Cu−ON configuration for state B, as considered as a secondary minimum in several theoretical studies.[5,8,9] Besides the fact that the harmonic frequencies for this form are predicted at much lower frequencies (about 1430, 330, and 195 cm^{-1}), it appeared clearly that the observed isotopic effects are not compatible with a Cu−O attachment. For instance, the larger ^{14}N/^{15}N and smaller ^{16}O/^{18}O isotopic effects on the ν_2 stretching mode near 512 cm^{-1} cannot be accounted for while the proper ^{63}Cu/^{65}Cu effect is maintained, even qualitatively (the trends are reversed by a factor of 3−4).

For both states, the normal coordinate description at this level indicates that the lowest frequency mode, ν_3, mainly implies the bending coordinate and ν_2 the Cu−N stretching one, but the relative weights are much closer for state A. For A, the N−O, Cu−N, and Cu−N−O force constants are on the order of 11.4 and 1.3 mdyn Å^{-1} and 0.53 mdyn Å rad^{-2}, respectively. For B, the N−O, Cu−N, and Cu−N−O force constants are on the order of 10.0 and 2.6 mdyn Å^{-1} and 0.28 mdyn Å rad^{-2}, respectively. It should be noted that in both states, the NO force constants are not very different (F_{NO} = 11.4 and 10.0 mdyn Å^{-1}), but in B the metal−nitrogen force constant is about twice that in A, while the bending force constant is half as much. Thus, the A and B states have practically the same bond angle, but the Cu−N force constants are very different, which indicates a substantial difference in bond lengths.

b. Electronic Spectra of CuNO. Conversion between A and B states of CuNO results from a photoexcitation in the visible or in the infrared, which promotes the complex to other excited electronic states. This process must involve one or several intermediate excited states, which can be characterized by recording absorption spectra of the (Cu + NO)/Ar and (Cu + NO)/Ne samples in the 5000−30 000 cm^{-1} spectral range.

Cu + NO in Neon. Figure 7 shows the spectrum obtained for Cu + NO deposits in Ne, where only one CuNO state was evidenced and vibrational levels are labeled with the (υ'_1,υ'_2,υ'_3) quantum numbers. Three vibrational progressions are distinguished due to increasing excitation of the three vibrational modes of CuNO in its first excited electronic state, in the 5000−8000 cm^{-1} spectral range. The strongest band at 5444.8 cm^{-1} corresponds to the vibrational origin in the vibronic system, as

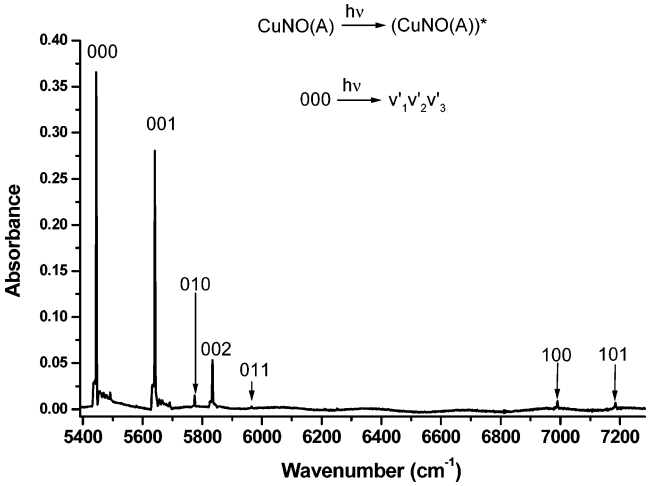

Figure 7. Electronic spectrum of CuNO in a neon matrix in the 5000−7500 cm^{-1} range.

TABLE 4: Observed Frequencies (cm^{-1}) for System C←A Vibronic Transitions of CuNO

electronic transition[a] $(v_1'',v_2'',v_3'') \rightarrow (v_1',v_2',v_3')$	$Cu^{14}N^{16}O$	$Cu^{15}N^{16}O$	$Cu^{14}N^{18}O$
(0,0,0) → (0,0,0)	5444.8	5447.4	5446.4
(0,0,0) → (0,0,1)	5641.3	5641.8	5636.7
(0,0,0) → (0,0,2)	5834.1	5833.8	5823.9
(0,0,0) → (0,1,0)	5774.3	5769.3	5774.5
(0,0,0) → (0,1,1)	5966.3	5958.8	5965.5
(0,0,0) → (1,0,0)	6990.2	6966.5	6950.9
(0,0,0) → (1,0,1)	7184.9	7159.3	7138.9
(0,0,0) → (1,0,2)	7374.4	7347.2	7322.6

[a] v''_1,v''_2,v''_3 and v'_1,v'_2,v'_3 refer to vibrational quantum numbers of ground and excited electronic states.

evidenced by the very small *blue* shifts observed with the heavier isotopic species, while all other bands present various amounts of *red* shifts.

Two transitions (0,0,0) → (0,0,*k*) are observed at 5641.3 and 5834.1 cm^{-1} for $k = 1$ and 2. These transitions give access to the lowest energy vibrational mode (ν_3) of the excited electronic state of CuNO. The transitions (0,0,0) → (0,1,*k*) involving the second mode (ν_2) are observed at 5774.3 and 5966.3 cm^{-1} for $k = 0$ and 1. Finally, the third mode (ν_1) is responsible for the (0,0,0) → (1,0,*k*) transitions, at 6990.2, 7184.9, and 7374.7 cm^{-1} for $k = 0$, 1, and 2.

These transitions were observed for the three isotopic species $Cu^{14}N^{16}O$, $Cu^{15}N^{16}O$, and $Cu^{14}N^{18}O$. Table 4 gathers frequencies of all observed electronic transitions between ground and excited-state C of the complex. The intensity for the whole vibronic system can be measured relative to the ν_1 fundamental and is found to be only 4 times as intense.

In the 15 000−20 000 cm^{-1} range, another absorption signal of CuNO is observed (Figure 8). In addition to the band attributed to Cu_2 species,[16] two broad absorptions around 17 000 and 18 500 cm^{-1} are assigned to CuNO, characterizing other excited electronic states. A clear sign of vibrational structure is observed, but the bands are too broad for characterization of these excited states. The only information is the energy range in which these excited electronic states can be accessed (2 and 2.4 eV) and the strong intensity (about 50 times stronger than the NIR transition) of these absorptions, which indicates that these are likely to be fully allowed, in contrast to the 5400 cm^{-1} system in the near-IR.

Cu + NO in Argon. The coexistence in the argon matrix of two nearly isoenergetic states A and B of CuNO might induce

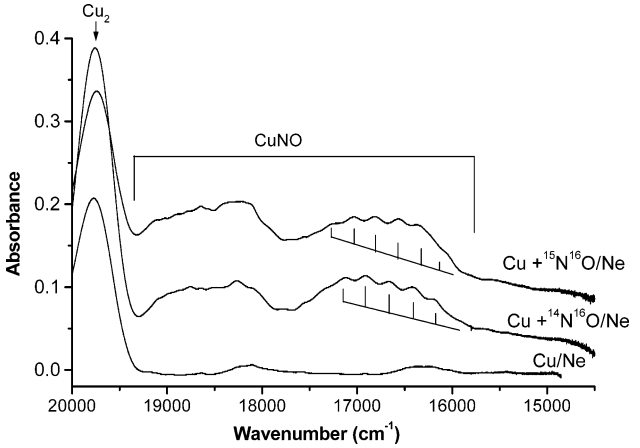

Figure 8. Electronic spectra in a neon matrix in the 15 000−20 000 cm^{-1} range: (a) Cu/Ne blank, (b) Cu + $^{14}N^{15}O$/Ne, (c) Cu + $^{15}N^{16}O$/Ne.

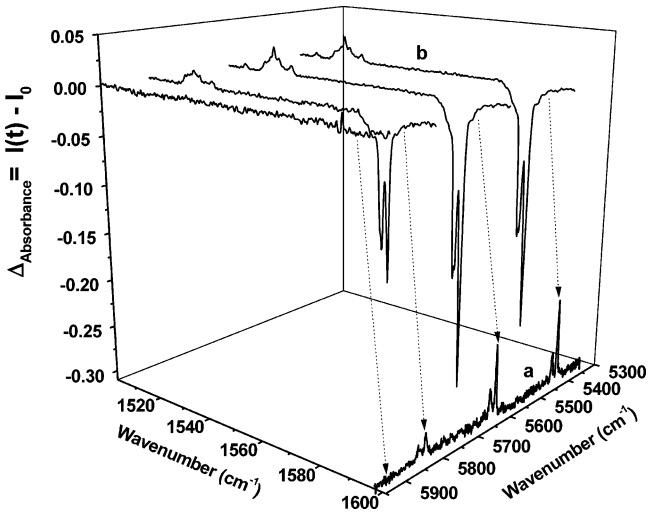

Figure 9. Selective photoirradiation process of CuNO in solid argon: (a) electronic spectrum of CuNO in the C ← A near-IR system, (b) difference IR spectra in the mid-IR nitrosyl stretching region. I_0, spectrum before irradiation, $I(t)$ spectrum immediately after 5 min irradiation at the selected wavenumbers indicated by arrows.

a different electronic spectrum from that obtained in neon. Insofar as the A and B states (singlet and triplet) coexist at low temperature, different excited states could be accessed in the singlet and triplet manifolds. However, the electronic spectrum obtained in the argon matrix is quite similar to that obtained in neon (in both 5000−8000 and 15 000−20 000 cm^{-1} regions). Only the bands are much broader than in neon, and as the medium is more scattering, only the strongest transitions were observed. No supplementary electronic transition originating from state B is observed.

A selective photoirradiation can be carried out, the electronic spectrum giving directly the transition wavelengths between ground and excited states. The sample is then irradiated by tuning the laser over wavelengths corresponding to the transitions (0,0,0) → (0,0,*k*) with $k = 0$, 1, and 2. Figure 9 shows the variation of the $v''_1 = 0 \rightarrow v''_1 = 1$ absorption bands of the NO stretching modes for states A and B according to laser excitation wavelengths. The variation of population of states A and B depends on the intensity distribution of the vibrational progressions in the electronic spectrum. By exciting CuNO with the (0,0,0) → (0,0,0) and (0,0,0) → (0,0,1) transitions near 5400 and 5600 cm^{-1} (trace 9a), the reduction of state A population and the increase in state B population is a maximum (traces in

TABLE 5: Observed and Calculated[a] Frequencies (cm^{-1}) for Isotopic Species of CuNO in the Electronic State C

	NO stretch		CuN stretch		CuNO bend	
CuNO (C)	exp	calc	exp	calc	exp	calc
$^{63}Cu^{14}N^{16}O$	1545.4	1545.4	329.5	329.5	196.2	196.1
$^{63}Cu^{15}N^{16}O$	1519.1	1518.3	321.9	321.9	194.6	194.0
$^{63}Cu^{14}N^{18}O$	1504.6	1503.8	328.2	328.1	190.6	189.6

[a] Using a semiempirical harmonic force field. The force constants are $F_{NO} = 10.8$ mdyn Å^{-1}, $F_{CuN} = 1.1$ mdyn Å^{-1}, $F_{CuNO} = 0.24$ mdyn Å rad^{-2}, $F_{NO,CuNO} = 0$ mdyn rad^{-1}, $F_{NO,CuN} = 0.9$ mdyn Å^{-1}, $F_{CuN,CuNO} = 0.25$ mdyn rad^{-1}. $r_{NO} = 1.17$ Å, $r_{CuN} = 1.94$ Å, $\angle CuNO = 120°$.

Figure 9b, arrows on the right). This variation is much less important when the laser wavelength is tuned on the transition (0,0,0) → (0,0,2) (third trace from right). No variation of population is measured when the sample is excited outside the CuNO electronic absorption range.

4. Discussion

The vibrational frequencies of the excited electronic state C are reported in Table 5 and compared with the frequencies calculated with the harmonic force-field approximation, using the same method and criteria as for the A and B states. Also, harmonic force-field calculations are in good agreement with the experimental results only when the CuNO bond angle in the excited electronic state (near 5000 cm^{-1}) is found around 120° ± 10° (recall that the A and B states have bond angles around 130 ± 10°). Comparing the force constants in the excited C and lower A and B states, the following trends are notable:

The force constant k_{NO} in C is close to the A and B state values.

The k_{Cu-N} force constant in C is half that in B and close to that of A.

The k_{CuNO} force constant is half that in A and close to that of B.

The vibrational progressions observed in ν_3 (predominantly the bending mode) in the electronic spectrum show, however, that the bond angle changes slightly between the ground and the excited electronic state. We simulated the electronic spectrum using a method developed by Smith, with second-order perturbation theory to derive the relative intensity distributions for vibrational progressions in electronic spectra, based on the harmonic approximation.[17] It requires the normal-mode frequencies involved in ground and excited states and estimates of the initial and final state equilibrium geometries. The first parameter is deduced from our experimental data and the second is varied to fit the experimental intensities of electronic spectrum. Figure 10 shows the change in predicted relative intensities in the vibrational progression while varying the difference in bond angle ($\Delta\theta$) between ground and excited states. These simulated spectra are compared to the experimental spectrum. A good agreement with the experimental observation is obtained when the difference in the bond angle between ground and excited states is taken very small, around 4°, consistent with the results of harmonic force-field calculations.

On the basis of our experimental findings and the existing theoretical calculations, possible descriptions of the conversion between A and B states are outlined in Figure 11 (Schemes 1 and 2). Populations P_A and P_B of A and B states can be determined by measuring relative intensity of their vibrational absorption bands. Photoexcitation to state C in the NIR or to higher energy states in the visible range, led to a reduction in P_A and an increase in P_B. Immediately after, a slow conversion (B → A) brings the system back to its starting populations. This

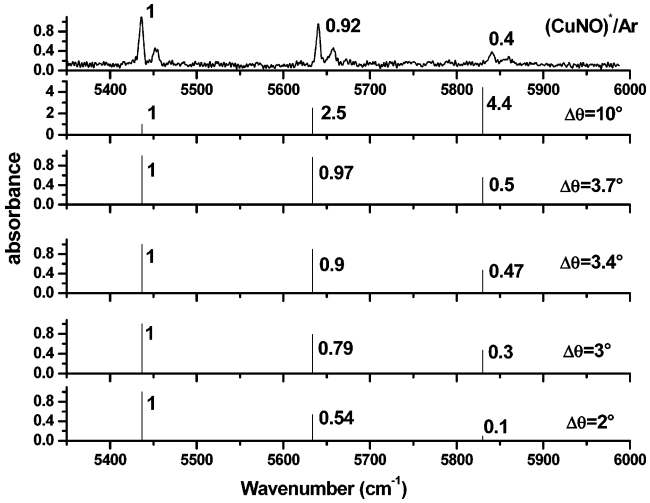

Figure 10. Comparison of experimental and simulated electronic vibronic spectrum of CuNO in solid argon: The values reported on each spectrum correspond to the intensities of each vibronic band, relative to the (0,0) origin.

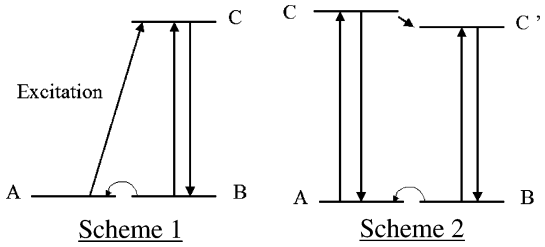

Figure 11. Suggested photoconversion schemes between the two low-lying states A and B.

process must involve one (Scheme 1) or several (Scheme 2) intermediate excited states.

Assuming first that state C has a different spin multiplicity than state A to explain the relatively low C ← A intensity, then B and C should be of the same multiplicity. It follows that the C ← B transition should be more favorable than C ← A, which corresponds to what is observed in the relaxation process (Scheme 1 in Figure 11). This offers, however, no obvious explanation for the absence of C ← B transition in the absorption spectrum in argon. Assuming second that state C and A are of the same multiplicity, one is led to consider a four-level scheme (Scheme 2 in Figure 11) in which matrix-induced nonradiative relaxation would lead to rapid population of a fourth state (C′) of the same multiplicity as state B, followed by radiative decay to B. The low intensity of the C ← A transition in excitation would then be due to a low electric dipole rather than to a spin-forbidden character. Fluorescence measurements might discriminate between the two possibilities, as the second scheme will produce a large red-shift in C′ → A emission following the initial C ← A excitation.

5. Conclusions

The vibrational and electronic spectra of the CuNO complex have been investigated in argon and neon matrixes. In argon, two very low lying electronic states, A and B, of CuNO have been observed. They are likely to correspond to the two low lying states, $^1A'$ and $^3A''$, respectively, considered in former theoretical studies. In neon, only state A is observed, and state B can be observed only if argon atoms are added in the neon matrix. Excitations in the visible or near-IR lead to photoconversion between the A and B states. Spontaneous conversion

of B toward A is then observed, the system returning slowly to its initial balance with first-order kinetics and an effective rate constant of 300 ± 10 s. Electronic spectra of the CuNO complex are recorded, on one hand to characterize this phenomenon and, on the other hand, to enable discussion of the vibrational modes and geometry of the next excited electronic state C of CuNO, observed 0.67 eV above the ground state.

Acknowledgment. We thank Danielle Carrère and Lucie Norel for their careful assistance in the experiments. This work was supported by CNRS-UPMC (UMR 7075), NSF (Grant CHE 00-78836) and Plan Pluri-Formation of the University Pierre et Marie Curie.

References and Notes

(1) Lambert, R. M.; Pacchioni, G. *Chemisorption and Reactivity on Supported Clusters and Thin Films;* Kluwer Academic Publishers: Dordrecht, 1997.
(2) Henry, C. R. *Surf. Sci. Rep.* **1998**, *31*, 231.
(3) Franck, M.; Kühnemuth, R.; Bäumer, M.; H. J. Freund, *Surf. Sci.* **2000**, *454*, 968.
(4) Süzle, D.; Schwarz, H.; Moock, K. H.; Terlouw, J. K. *Int. J. Mass Spectrom. Ion Proc.* **1991**, *108*, 269.
(5) Hrusak, J.; Koch, W.; Schwarz, H. *J. Chem. Phys*. **1994**, *101*, 3898.
(6) Chiarelli, J. A.; Ball, D. W. *J. Phys. Chem. A* **1994**, *98*, 12828.
(7) Ruschel, G. K.; Nemetz, T. M.; Ball, D. W. *J. Mol. Struct.* **1996**, *384*, 101.
(8) Zhou, M. F.; Andrews, L. *J. Phys. Chem. A* **2000**, *104*, 2618.
(9) Barone, V.; Adamo, C. *J. Phys. Chem* **1996**, *100*, 2094.
(10) Blanchet, C.; Duarte, H.; Salahub, D. *J. Chem. Phys*. **1997**, *106*, 8778.
(11) Manceron, L.; Alikhani, M. E.; Tremblay, B. *J. Phys. Chem. A* **2000**, *104*, 3750.
(12) Clusius, K. *Angew. Chem*. **1954**, *66*, 497.
(13) Andrews, L.; Citra, A. *Chem. Rev*. **2002**, *102*, 885.
(14) Krim, L.; Alikhani, M. E.; Manceron, L. *J. Phys. Chem. **A***, **2001**, *105*, 7812.
(15) Alikhani, M. E.; Krim, L.; Manceron. L. *J. Phys. Chem. **A*** **2001**, *105*, 7817.
(16) Kolb, D. M.; Rotermund, H. H.; Schrittenlacher, W.; Schroeder, W. *J. Chem. Phys*. **1984**, *80*, 695.
(17) Smith, W. L. *J. Mol. Spectosc.* **2003**, *225*, 39.